Geophysical Research Letters, 22(11), 1413-16, 1995

Quantitative Visualization of Entrapped Phase Dissolution Within a Horizontal Flowing Fracture

R.J. Glass and M.J. Nicholl

Geohydrology Department 6115, Sandia National Laboratories, Albuquerque, New Mexico

Abstract. An experiment was conducted to demonstrate the utility of quantitative fracture flow visualization techniques in the study of entrapped fluid phase (air) dissolution into a flowing phase (water) within a horizontal, transparent, analog rough-walled fracture. The fracture aperture field and phase occupancy were measured using light transmission techniques and then combined to calculate bulk water-phase saturation within the fracture as a function of time. Fracture relative permeability as a function of water-phase saturation showed a smooth power law behavior during dissolution. Periodic step pulses of clear water within the dyed water inflow yielded dye concentration fields that demonstrate channeling induced by the entrapped air phase. Clusters of the entrapped air-phase exhibited three types of dissolution behavior: general shrinkage, interfacial recession along cluster appendages, and cluster splitting. Locations for the advance of the wetting phase (water) into a nonwetting entrapped air cluster on its dissolution are not always correlated with either zones of high mass transfer rate (as inferred from gradients in the pulsed dye concentration fields) or with narrow apertures where the wetting phase has been thought to most easily invade. These results suggest that within an individual cluster of the entrapped phase, fluid pressure is at equilibrium and that the path of cluster shrinkage may be controlled primarily by capillary forces resulting from the full three-dimensional curvature that minimizes surface energy of the phase interface.

Introduction

Dissolution of an entrapped fluid phase within a flowing fracture is an important process with implications for various applied problems, ranging from the extraction of hydrocarbon contaminants in fractured rock below the water table to post-waste emplacement gas dissolution in the vicinity of a high level radioactive waste repository situated in regionally saturated fractured rock. While entrapped or "residual" phase dissolution in porous media has been studied (e.g., Geller and Hunt, 1993; Imhoff et al., 1994), we are unaware of any investigations of phase dissolution in fractured rock.

Consider a two-phase system within a rough-walled, flowing fracture in which the viscous forces associated with the flowing phase are insufficient to overcome the capillary forces pinning the entrapped phase in place. Under such conditions, entrapped phase extraction is limited to dissolution into the flowing phase. Dissolution rate will be dependent on: local entrapped phase concentration gradients within the flowing phase, the ratio of interfacial area to entrapped phase volume, geometry of the entrapped phase, and structure of the flow field within the fracture.

In this paper, we demonstrate the utility of quantitative visualization techniques for systematic investigation of entrapped phase dissolution within a flowing fracture. By passing visible light through a transparent analog fracture and exploiting differences in light absorbency between the various experimental fluids, we are able to collect detailed spatial and temporal data regarding system behavior including phase occupancy and flow field structure. Our flow system consists of a homogeneous, isotropic analog fracture in which the non-wetting phase (air) is entrapped by the flowing wetting phase (water). Reflecting the target scenario for time-effective remediation schemes, flow rates were maintained sufficiently high as to keep the flowing phase under-saturated with respect to the entrapped phase.

Experimental Design

Light transmittal through a horizontally oriented, transparent analog fracture is measured using a high resolution (~2000 by ~2000 pixels) digital imaging system and analyzed to quantify aperture field structure, phase occupancy, and dye tracer concentration at ~0.15 mm spatial resolution with 12 bit dynamic range (4096 gray levels). The analog fracture (mean aperture = 0.02 cm, saturated hydraulic conductivity = 3.13 cm/sec, and fracture/water/air contact angle = 35 degrees) is formed by holding two plates of roughened glass (15 x 30 cm) in contact. Normal pressure (20 psi) is applied to remove long wavelength perturbations and assure a reproducible aperture field. Correlation length of the resultant aperture field (ρ = 0.07 cm), is over two orders of magnitude smaller than system scale. Long sides of the fracture are sealed, inlet and outlet manifolds on the ends are connected to manometers for measurement of differential pressure head and mass flow rate is measured gravimetrically at the outflow boundary. Pulses of clear water are used to visualize the flow field; sharp transitions between the dyed and clear fluids are implemented with computer controlled solenoid valves. For more details on the analog fracture, test cell, transmitted light imaging system, and data reduction algorithms see Nicholl and Glass (1994).

The experimental sequence began with measurement of the aperture field using the matched index of refraction, light adsorption technique (Nicholl and Glass, 1994). The horizontal fracture was then saturated with dyed (FD&C blue #1), air-equilibrated water and saturated permeability of the fracture measured. Air was then slowly injected through the inlet manifold until breakthrough at the outlet. The complicated air invasion structure that resulted contained many entrapped water clusters at a variety of sizes. Following air breakthrough, the fluid supply was switched to steady injection of air-equilibrated dyed water (5.5 ml/min). The phase structure adjusted

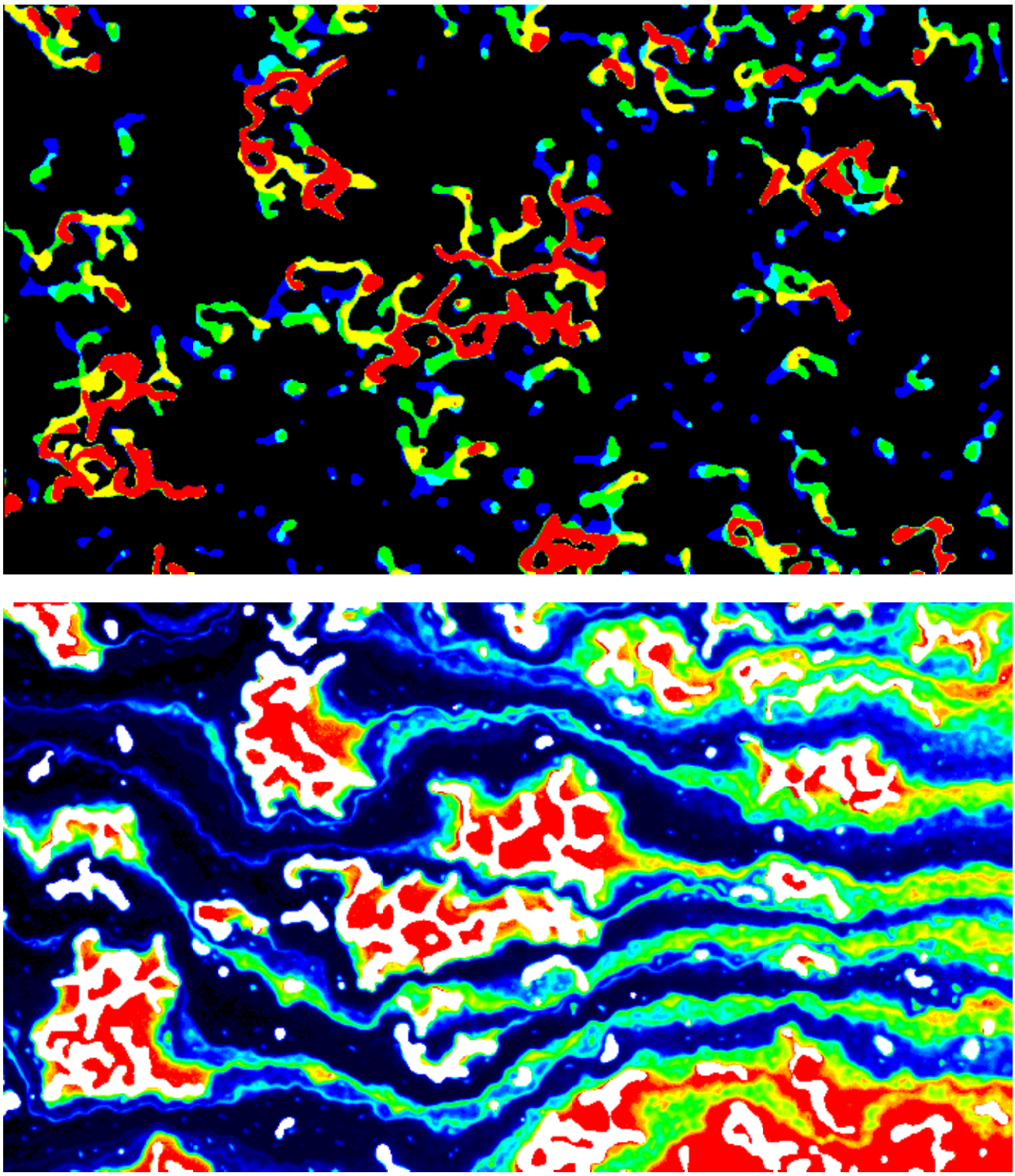

Figure 1. Composite dissolution image and channelization visualization: Experimental data was analyzed to build composite dissolution (top) and relative concentration (bottom) images; for clarity only a 5.8 x 10.2 cm region of the 15 x 30 cm experiment is displayed, with flow from left to right. The composite dissolution image (top) shows the dissolution process from t = 0 min through the end of the experiment (t = 231 min). Regions where no change in phase saturation occurred are displayed as black (water) and red (air). Regions where dissolution resulted in the replacement of air by water at intermediate times during the experiment are shown as violet (t = 0 - 25), blue (t = 25 - 73), green (t = 73 - 141), and yellow (t = 141 - 231). Dyed water within the fracture is displaced by clear water from left to right in order to visualize the flow field at t = 23 min (bottom). The inlet manifold was flushed to provide a sharp transition between fluids. The relative dye concentration field (from 0 to 1), is depicted by the standard color bar (black (0)-blue-green-yellow-red(1)); in the bottom figure, white denotes the entrapped air phase.

to accommodate the flowing water phase, entrapping the non-flowing air phase in a complicated field composed of clusters exhibiting a wide range of sizes.

The dissolution test was begun by switching flow to dyed de-aerated water (also 5.5 ml/min). Differential pressure head and digital images of the experiments were recorded in time. At 20 minute intervals, the flowing fluid was changed across the full width of the inlet manifold to clear air-equilibrated water and then after 3 minutes, back to the dyed de-aerated water. Differences in light absorption between the clear and dyed fluids during this clear pulse facilitated visualization of flow channels induced by the phase structure and allowed observation and measurement of mixing processes along the clear/dyed water interface. The experiment lasted a total of 231 minutes; data collection was interrupted from t = 73 - 141 minutes in order to download data. Raw images were processed to yield phase occupancy fields using the method of Nicholl and Glass (1994) and relative dye concentration fields using the method of Norton and Glass (1993).

Results

The entrapped phase structure at the beginning of dissolution consisted of 688 clusters ranging from very small bubbles on the order of ρ to large, complicated features roughly 50 times ρ, all of which were distributed about the fracture in a fairly uniform manner. Liquid permeability in this phase structure was reduced from the saturated case by more than a factor of 4, demonstrating a dramatic increase in flow field complication (tortuosity) induced by an entrapped phase structure consistent with that observed by Nicholl and Glass (1994). Liquid saturation was defined as the fraction of the aperture volume occupied by the wetting phase (water) and was measured by coupling the measured phase occupancy structure with the aperture field.

Changes in phase occupancy structure over time were visualized by overlaying the phase structure measured at 5 intervals spanning the experiment to form a composite image; a portion of this composite image is shown in Figure 1 (top). In general, small clusters were observed to dissolve first and large ones last. However, the behavior of individual entrapped phase clusters during dissolution appeared to be a function of cluster size. Small clusters (on the order of ρ) tended to simply shrink in a relatively uniform manner, while somewhat larger clusters (an order larger than ρ) first exhibited interfacial recession along cluster appendages, followed by uniform shrinkage. The largest clusters were occasionally observed to split into smaller features.

The average liquid saturation profile was measured from inlet to outlet along 1950 full-width scan lines oriented perpendicular to the imposed gradient. Positions of initially low saturation correspond to the presence of large entrapped clusters. Flow visualization (pulses of clear water) showed these large clusters to significantly channel flow and define the primary flow channels (see Figure 1, bottom). Because the largest entrapped clusters were the last to dissolve, these primary channels remained persistent during dissolution. As dissolution progressed, smaller channels caused by small entrapped regions within the major channels were observed to merge and straighten out. Dissolution also smoothed the average liquid saturation profile by dissolving regions of low saturation roughly twice as fast as those of high saturation. This observation is expected since high mass transfer rates should be associated with the high velocities induced by flow convergence. Dissolution rates do not show a decreasing trend from inlet to outlet, confirming that solving strength of the flowing phase did not diminish as it passed through the fracture.

Wetting-phase relative permeability (k_r), defined as the ratio of permeability measured under partially saturated conditions to that measured under fully saturated conditions, appears to display a power law relationship with liquid saturation ($k_r \sim S^n$, with n ~5, see Figure 2). Measured k_r was observed to increase smoothly during dissolution, reflecting the observations made above that dissolution acted to refine the flow structure rather than inducing abrupt changes in flow path.

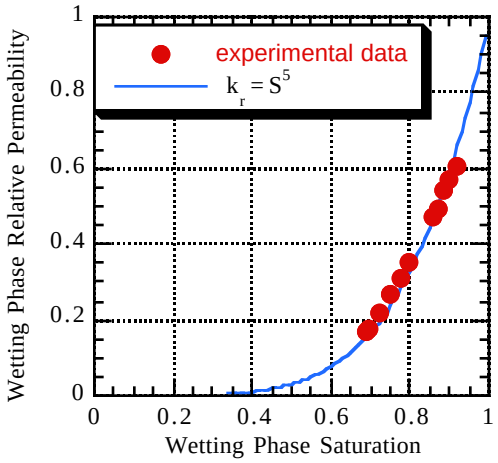

Figure 2. Relative permeability during dissolution.

Comparison to simple conceptual models for entrapped cluster dissolution

One might expect dissolved entrapped fluid to be replaced with the solvent fluid at locations of high mass transfer rate (e.g., large concentration gradient within the solvent fluid adjacent to an entrapped cluster). Alternatively, if phase replacement is a function of capillary pressure, either standard percolation (e.g., Pruess and Tsang, 1990) or standard invasion percolation models (e.g., Mendoza, 1992) may apply.

Expected regions for high inter-phase mass transfer rates were inferred by applying a scalar gradient operator to relative dye concentration fields measured using the flow visualization periods. Delineating regions around entrapped clusters where this gradient is highest allows us to predict where the highest inter-phase mass transfer rates should occur. It was observed that clusters do not necessarily shrink at the points of highest mass transfer rates (e.g., compare Figure 1, top and bottom). This lack of agreement suggests that the fluid pressure within an individual entrapped fluid cluster is near equilibrium.

Percolation approaches are based on an assumption of near equilibrium pressures within each phase. The validity of such

models in predicting phase replacement can be explored by examining the aperture field associated with each cluster to determine the order in which apertures should fill with water as dissolution progresses. Both standard percolation and standard invasion percolation rules that use the local aperture as the sole basis for determining phase entry order were considered. Neither approach was consistent with experimental observations; clusters did not necessarily shrink at the points predicted by either of these models. As an illustrative example, Figure 3 shows the results of standard percolation applied to a single representative cluster from Figure 1 (top).

This lack of agreement between standard models and our data suggests that each cluster and its path of shrinkage may be controlled by capillary forces resulting from the fully three-dimensional curvature at the phase interface that acts to minimize surface energy. Modification of invasion percolation to include the neglected in-plane radius of curvature and local divergence and convergence angles of the fracture surfaces was presented by Glass (1993). In that study, comparison of the modified invasion percolation model to data from gravity-driven fingering experiments conducted at the quasi-static limit showed good agreement.

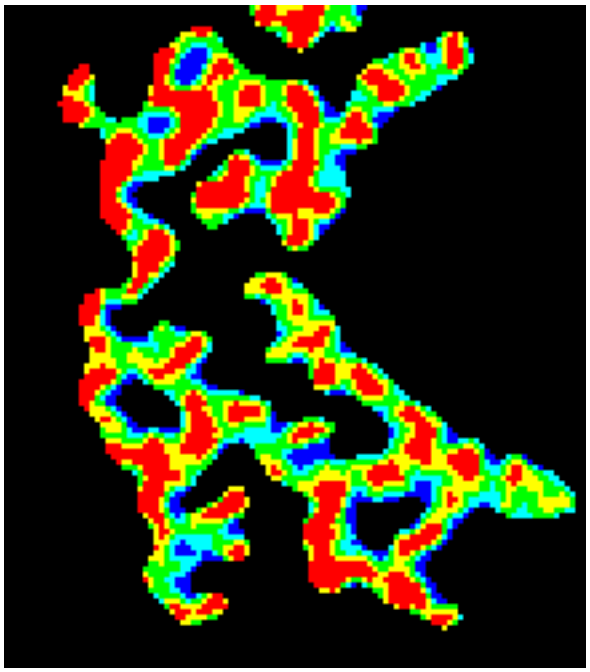

Figure 3. Comparison to Percolation Models: Measured aperture of a typical cluster in the upper left quadrant of Figure 1 were used to explore simulation of dissolution using standard percolation theory. The order of water-phase displacement, depicted by color scale as in Figure 1 (top), is shown to be very different from reality (note magnification of 2.5 here over that in Figure 1).

Conclusion

The work presented here serves as a basis for additional systematic explorations necessary to understand entrapped phase dissolution in fractures. The entrapped phase structure will be a function of boundary conditions, initial conditions, and fracture inclination (Nicholl et al., 1993, Nicholl and Glass, 1994). Since both the relative permeability and the path of dissolution will be a function of the initial entrapped structure, variation in the initial phase structure must be considered systematically. In addition, the work presented here considered flow rates that were sufficiently high as to keep the flowing phase under-saturated with respect to the entrapped phase. At much lower flow rates, the solvent fluid will become saturated with the entrapped phase along its flow path. Standard (1-D) analysis of this situation assuming a "homogeneously" distributed entrapped phase yields a sharply defined dissolution front that moves through the system from inflow to outflow. Based on our observations of flow channelization induced by what in reality is a heterogeneous field formed by entrapped phase clusters of various sizes, a dissolution front will likely be less sharp (in a one-dimensional sense) than previously expected. Finally, the influence of aperture field structure (variability, correlation length) on entrapped phase dissolution must be determined so that results may be applied to the wide variety of fractures expected in natural systems.

Acknowledgments. This work was supported by the U.S. Department of Energy under contract DE-AC04-94AL85000, through the Office of Civilian Radioactive Waste Management, Office of Program Management and Integration, International Programs, WBS 9.3.3.2.2.

References

Geller, J.T., and J.R. Hunt, Mass Transfer From Nonaqueous Phase Organic Liquids in Water-saturated Porous Media, *Water Resources Res.*, 24(4), 833-845, 1993.

Glass, R.J., Modeling Gravity-Driven Fingering Using Modified Percolation Theory, *Proc. 4th Ann. Int. Conf. on High Level Rad. Waste Mgmt.*, Am. Nuc. Soc., Las Vegas, Nevada, April 26-30, 2042-2052, 1993.

Imhoff, P.T., P.R. Jaffe, and G.F. Pinder, An Experimental Study of Complete Dissolution of a Nonaqueous Phase Liquid in Saturated Porous Media, *Water Resources Res.*, 30(2), 307-320, 1994.

Mendoza, C.A., Capillary Pressure and Relative Transmissivity Relationships Describing Two-phase Flow Through Rough-walled Fractures in Geologic Materials, Ph.D. dissertation, University of Waterloo, Waterloo, Ontario, Canada, 1992.

Nicholl, M.J., and R.J. Glass, Wetting Phase Permeability in a Partially Saturated Horizontal Fracture, *Proc. 5th Ann. Int. Conf. on High Level Rad. Waste Mgmt.*, Am. Nuc. Soc., Las Vegas, Nevada, May 22-26, 2007-2019, 1994.

Nicholl, M.J., R.J. Glass, and H.A. Nguyen, Wetting Front Instability in an Initially Wet Unsaturated Fracture, *Proc. 4th Ann. Int. Conf. on High Level Rad. Waste Mgmt.*, Am. Nuc. Soc., Las Vegas, Nevada, April 26-30, 2061-2070, 1993.

Norton, D.L., and R.J. Glass, Full-field Dye Measurement Within Saturated/Unsaturated Thin Slabs of Porous Media, *Proc. 4th Ann. Int. Conf. on High Level Rad. Waste Mgmt.*, Am. Nuc. Soc., Las Vegas, Nevada, April 26-30, 1993, 1066-1075, 1993.

Pruess,. K., and Y.W. Tsang, On Two-Phase Relative Permeability and Capillary Pressure of Rough-Walled Rock Fractures, *Water Resources Res.*, 26(9), 1915-26, 1990.

R.J. Glass, Sandia National Laboratories, Geohydrology Dept. 6115, MS-1324, Albuquerque, NM 87185. (e-mail: rjglass@nwer.sandia.gov)
M.J. Nicholl, Sandia National Laboratories, Dept. 6115, MS-1324, Albuquerque, NM 87185. (e-mail: mjnicho@nwer.sandia.gov)